# Fabrication and performance optimization of Mn–Zn ferrite/EP composites as microwave absorbing materials*

Wang Wen-Jie(王文杰), Zang Chong-Guang(臧充光)†, and Jiao Qing-Jie(焦清介)

*State Key Laboratory of Explosive Science and Technology, School of Mechanical Engineering, Beijing Institute of Technology, Beijing* 100081, *China*

(Received 6 June 2013; revised manuscript received 6 August 2013)

Magnesium-substituted $Mn_{0.8}Zn_{0.2}Fe_2O_4$ ferrite is synthesized by the sol–gel combustion method using citrate acid as the complex agent. The electromagnetic absorbing behaviors of ferrite/polymer coatings fabricated by dispersing Mn–Zn ferrite into epoxy resin (EP) are studied. The microstructure and morphology are characterized by X-ray diffraction and scanning electron microscope. Complex permittivity, complex permeability, and reflection loss of ferrite/EP composite coating are investigated in a low frequency range. It is found that the prepared ferrite particles are traditional cubic spinel ferrite particles with an average size of 200 nm. The results reveal that the electromagnetic microwave absorbing properties are significantly influenced by the weight ratio of ferrite to polymer. The composites with a weight ratio of ferrite/polymer being 3:20 have a maximum reflection loss of –16 dB and wide absorbing band. Thus, the Mn–Zn ferrite is the potential candidate in electromagnetic absorbing application in the low frequency range (10 MHz–1 GHz).

**Keywords:** ferrite, composite material, microwave absorber

**PACS:** 81.05.Zx, 72.80.Tm, 77.55.fj **DOI:** 10.1088/1674-1056/22/12/128101

## 1. Introduction

Recently, electromagnetic interference has attracted much attention due to the explosive growth in the utilization of electronic devices.[1,2] Electromagnetic absorbing material can reduce or weaken the electromagnetic interference signals and therefore is very important. In this field, ferrite is a kind of desired material, owing to its big magnetic moment and high resistivity. The spinel ferrite, such as Mn–Zn ferrite, exhibits magneto–optical property and well matched magnetic and dielectric properties.[3,4] It can be synthesized by the traditional co-precipitation method, ceramic method, combustion method, and hydrothermal processing.[5–8] However, these methods can result in poor compositional control, size inhomogeneity, and phase impurity. Han and Deng,[9] Yu *et al.*,[10] Ren and Zhang,[11] and Tian *et al.*[12] also have reported that the magnetic properties of the magnetic materials considerably depended on their shapes, structures, and doped metals. In order to obtain the ferrite with good properties, an appropriate preparation method must be used. The sol–gel combustion method is one of the most promising processes due to its accurately controlled stoichiometric ratio and simple preparation technique.[13] It also has the advantages of homogeneous formation, high purity, and good crystalline structure.

Fabrication of ferrite/polymer composite coating has been proved to be a cost-effective and simple process.[14–16] Among the polymers, epoxy resin has aroused a great deal of interest due to the fact that it has unique behaviors in terms of good mechanics and excellent transparency and it still possess the properties of conventional polymers such as flexibility and easy solidify. Although most ferrite/polymer coatings have shown electromagnetic wave absorption and shielding properties, their performances are displayed often in a high frequency range.[17,18]

We use the facile sol–gel combustion method to synthesize and characterize the magnetic Mn–Zn ferrite. The microstructure and morphology of the prepared ferrite are investigated by X-ray diffraction (XRD) and scanning electron microscope (SEM). The reflection loss of ferrite/EP composite coatings is tailored by controlling the match between complex permittivity and permeability resulting from the weight ratio of ferrite to polymer.

## 2. Experiment

An aqueous solution was prepared by dissolving the manganese chloride, iron nitrate, and zinc nitrate which were weighted according to the stoichiometric proportion ($Mn_{0.8}Zn_{0.2}Fe_2O_4$) in deionized water with continuous stirring. Citrate acid was added into the aqueous solution with 1:1 molar ratio to metal and then mixed homogeneously with a magnetic stirring. Ammonia solution was added drop by drop for tuning the pH to about 7. The final obtained solution was heated at 90 °C for 6 h to achieve the wet gel. Then, the wet gel was heated at 100 °C for 2 h, and after that, cooled down to room temperature to obtain a dry gel. Finally, the dry gel was sintered at 1000 °C for 2 h to obtain dark grey branched powders.

*Project supported by the Specialized Research Fund for the Doctoral Program of Higher Education of China (Grant No. 20121101110014).

†Corresponding author. E-mail: zangchongguang@bit.edu.cn

© 2013 Chinese Physical Society and IOP Publishing Ltd 

The ferrite/EP composite coatings were fabricated by introducing the Mn–Zn ferrite into epoxy resin and curing agent mixture with different weight ratios and then stirred homogeneously at 60 °C. After that, the mixture was poured into the designed mould and then cured at 60 °C for 2 h for the characterization of electromagnetic properties. The samples of complex permittivity and permeability were prepared to form a circular disk with 2 cm in diameter and 2 mm in thickness, and a ring with 2 cm in the outer diameter, 0.5 cm in the inner diameter, and 2 mm in thickness, respectively. For the reflection loss sample, the mixed liquid was poured in a circular, disk-shape with 133 mm in diameter and 2 mm in thickness and four 5-mm-diameter holes.

XRD was used to investigate the microstructure of synthesized ferrite with Cu K$\alpha$ radiation. The morphology and particle size were characterized by SEM. The complex permittivity and permeability of the prepared ferrite/EP composite coatings were measured by an impedance analyzer (Agilent E4991A: 10 MHz to 1 GHz). The reflection losses of the composite coatings were characterized by a network analyzer (Agilent E5062A: 10 MHz to 1 GHz) using the transmission line method.

## 3. Results and discussion

The XRD patterns for the synthesized $Mn_{0.8}Zn_{0.2}Fe_2O_4$ spinel ferrite powders are shown in Fig. 1. The products are identified to be mainly $Mn_{0.8}Zn_{0.2}Fe_2O_4$ at [3 1 1], [4 4 0], [2 2 0], [4 3 0], [2 1 0] and confirmed to be cubic crystal which is in accordance with the JCPDS standard card.[19] It indicates that the sol–gel combustion reaction is almost completed. It can also be observed that it contains a small amount of $\gamma$-$Fe_2O_3$ due to the crystal transformation of $Mn_{0.8}Zn_{0.2}Fe_2O_4$ at a high temperature.[20]

Figure 2 displays the morphologies of $Mn_{0.8}Zn_{0.2}Fe_2O_4$ spinel ferrite. Figure 2(a) shows the loosely branched powder with a large number of microscopic pores due to the combustion propagating rapidly. Figure 2(b) shows that particles are Mn–Zn ferrite particles with typical cubic spinel shapes and the average particle size calculated from the SEM image is approximately 200 nm. It indicates that the spinel ferrite particles are homogeneous crystals and a narrow distribution of sizes, which is consistent with the analysis of XRD.

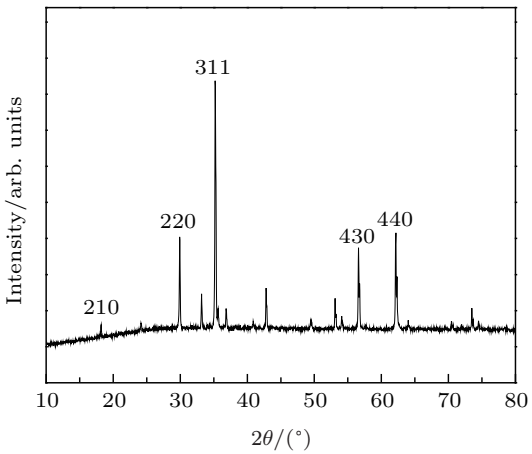



**Fig. 1.** XRD pattern of prepared ferrite $Mn_{0.8}Zn_{0.2}Fe_2O_4$.

The complex permittivity ($\varepsilon = \varepsilon' - j\varepsilon''$) of Mn–Zn ferrite/EP composite coatings is investigated as ferrite-to-polymer ratio (sample a: 1:200; sample b: 1:20; sample c: 3:20; sample d: 5:20; sample e: 7:20; sample f: 9:20) versus frequency. Figure 3 shows the variations of complex permittivity and dielectric loss angle tangent ($\tan\delta_\varepsilon = \varepsilon''/\varepsilon'$) with frequency. As shown in Fig. 3, the real part of the complex permittivity increases with the increase in weight ratio of ferrite to polymer. The dipole polarization and interfacial polarization between the contiguous particles which were separated by the epoxy resin result in a high value of dielectric constant.[21,22] The higher dielectric constant is attributed to more polarization resulting from the greater number of ions when the weight ratio of ferrite to polymer is high. It also displays that the imaginary parts of samples c–f are higher. The imaginary part of complex permittivity is due to the relaxation in polarization and the heterogeneity. The lag in polarization

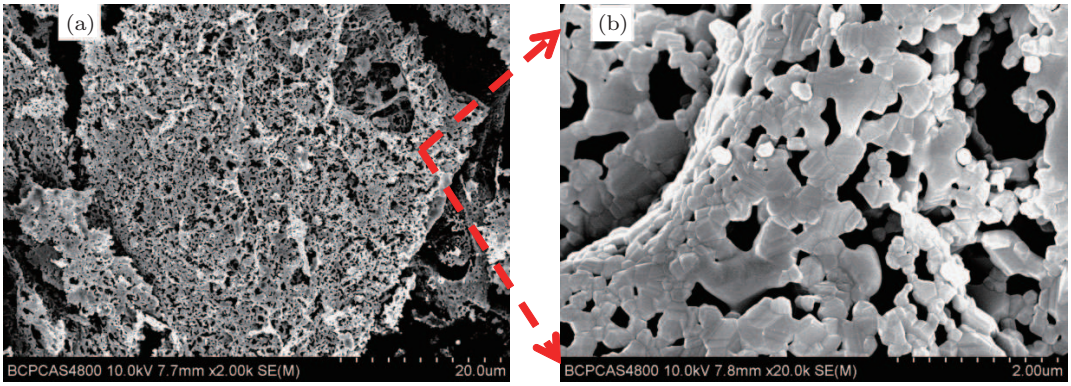



**Fig. 2.** (color online) SEM morphologies of $Mn_{0.8}Zn_{0.2}Fe_2O_4$, (a) the loosely branched powder; (b) the magnified image of the selected area.

is attributed to the externally applied electric field and the electron hopping between $Fe^{3+}$ and $Fe^{2+}$.[23] The heterogeneous mixture is a result of the ferrite weight ratio increasing with the decrease in homogeneity of the composite. As an absorbing material, the dielectric loss angle tangent represents the dielectric loss ability of the material for the electromagnetic wave. It is found that dielectric loss angle tangents of samples c and f are higher, resulting from the good matching between the real part and imaginary part of complex permittivity.

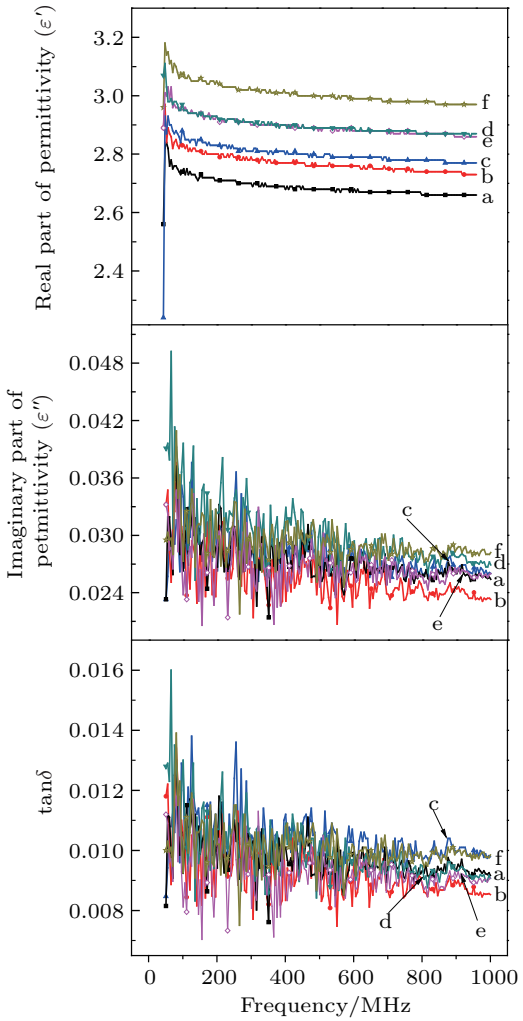



**Fig. 3.** (color online) Real and imaginary parts of complex permittivity, and dielectric loss tangent angle versus frequency for $Mn_{0.8}Zn_{0.2}Fe_2O_4$ with different weight ratios of ferrite/polymer (sample a: 1:200; sample b: 1:20; sample c: 3:20; sample d: 5:20; sample e: 7:20; sample f: 9:20).

Figure 4 shows the complex permeability ($\mu = \mu' - j\mu''$) spectra. Generally, almost for all samples, the values of $\mu'$, $\mu''$, and magnetic loss angle tangent ($\tan\delta_\mu = \mu''/\mu'$) increase with the increase of frequency for different weight ratios of ferrite to the polymer (a: 1:200; b: 1:20; c: 3:20; d: 5:20; e: 7:20; f: 9:20). The real part of complex permeability ($\mu'$) shows a minimum value at about 100 MHz. Both the imaginary part of complex permeability ($\mu''$) and the magnetic loss angle tangent decrease sharply below 100 MHz and then maintain the fluctuation condition with a low value. Both the real part and the imaginary part of complex permeability increase with the increase in content of ferrite according to Abbas *et al.*[21] In addition, the imaginary part of complex permeability and magnetic loss angle tangent are enhanced as a result of the relaxation in magnetization due to the applied external alternating field and the ferromagnetic resonance and domain wall resonance induced by the crystal anisotropy ($H_A$)[24,25]

$$H_A = \frac{2K}{M_s}, \tag{1}$$

where $K$ is the crystalline anisotropy constant and $M_s$ is the saturated magnetization of the material which is inversely proportional to the coercive force. The resonance increases with the increase of coercive force. Therefore, the magnetic loss ability is proportional to the content of ferrite in composite coating.

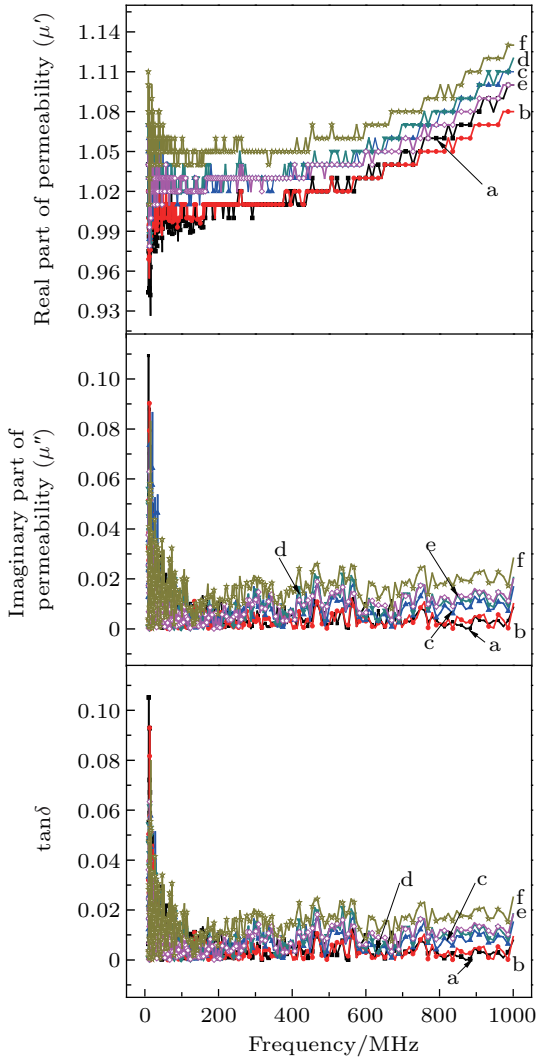



**Fig. 4.** (color online) Real and imaginary parts of complex permeability, and magnetic loss tangent angle versus frequency for $Mn_{0.8}Zn_{0.2}Fe_2O_4$ with different weight ratios of ferrite/polymer (sample a: 1:200; sample b: 1:20; sample c: 3:20; sample d: 5:20; sample e: 7:20; sample f: 9:20).

Figure 5 shows the electromagnetic wave absorbing characteristics. The input impedance of the absorbing coating can be defined by the equation:[23]

$$Z_{\text{in}} = Z_0 \sqrt{\frac{\mu}{\varepsilon}} \tanh\left[\frac{\mathrm{j}2\pi d}{\lambda}\sqrt{\varepsilon\mu}\right], \tag{2}$$

where $Z_0$ ($Z_0 \approx 377\ \Omega$) is the characteristic impedance of free space; the $\varepsilon$ and $\mu$ are complex permittivity and complex permeability, respectively; $d$ is the thickness of the prepared composite coating. The reflection loss of the composite coatings can be expressed according to the transmission line theory as:[23]

$$RL(\text{dB}) = 20\log\left|\frac{Z_{\text{in}} - Z_0}{Z_{\text{in}} + Z_0}\right|. \tag{3}$$

The perfect absorbing property is $Z_{\text{in}} = Z_0$ when the complex permittivity is well matched with the complex permeability.

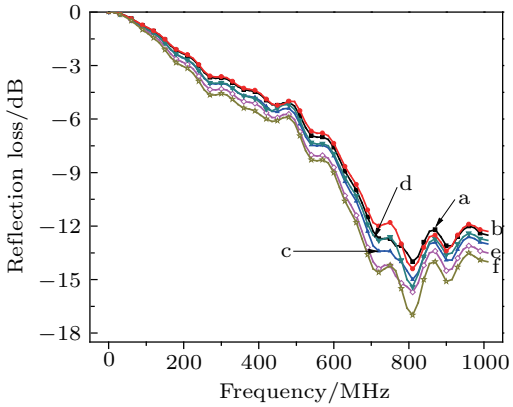



**Fig. 5.** (color online) Reflection losses versus frequency for $Mn_{0.8}Zn_{0.2}Fe_2O_4$ with different weight ratios of ferrite/polymer (sample a: 1:200; sample b: 1:20; sample c: 3:20; sample d: 5:20; sample e: 7:20; sample f: 9:20).

Figure 5 shows the absorption spectra for samples a–f. It is found that the reflection losses of samples a and b are smaller than those of other samples, while the reflection losses of samples e and f are bigger. The maximum reflection losses of samples a and b are smaller than –14 dB, yielding lower absorbing properties than others. Although the maximum reflection losses of samples e and f are bigger, it is not suitable for the absorbing coatings due to the large density of the coating. The reflection loss of sample c is bigger than those of samples a, b, and d with the maximum value nearly –16 dB at 800 MHz and the broad absorbing band with a minimum absorption of 10 dB from 700 MHz to 1 GHz.

In conclusion, it is worthwhile to discuss the technical utilization of the fabricated Mn–Zn ferrite and epoxy resin composite coatings. On the one hand, as an absorbing material, the reflection loss and absorbing band play an important role in obtaining the big value of reflection and wide absorbing frequency band. Our research results indicate that samples c, e, and f are suitable for the electromagnetic absorbing application. On the other hand, our research focuses on the potential applications of coatings in a low frequency range, which can function as absorbing material to protect the electrical devices and human body from being influenced by the electromagnetic radiation. We expect that this type of composite coatings will reduce the electromagnetic interference and possess the performances of low density, light weight, and better mobility. For samples e and f, it is hard to form uniform coating for the big content. Thus, the Mn–Zn ferrite/EP composite coating with 3:20 weight ratio of ferrite to the epoxy resin (sample c) can potentially be used in the electromagnetic absorbing field, owing to its lighter density, higher reflection loss, and wide absorbing band in a low frequency range.

## 4. Conclusions

In this work, we design and synthesize spinel ferrite $Mn_{0.8}Zn_{0.2}Fe_2O_4$ by the sol–gel combustion method. Mn–Zn ferrite particles are introduced into epoxy resin to fabricate the composite coatings. XRD and SEM reveal the typical spinel crystalline structure of Mn–Zn ferrite particles with an average size of 200 nm. Compared with the absorption ability of other absorbing composite coatings, strong absorbing ability with light density occurs when the weight ratio of ferrite to epoxy resin is 3:20. A good match between complex permittivity and complex permeability results in strong absorption and a broad absorbing band. Therefore, the prepared Mn–Zn ferrite/EP composite coatings show their potential as electromagnetic absorbing material in a low frequency range of 10 MHz–1 GHz.

## References

[1] Yang X C, Liu R J, Shen X Q, Song F Z, Jing M X and Meng X F 2013 *Chin. Phys. B* **22** 058101
[2] Wang W J, Jiao Q J, Zang C G and Zhu X D 2011 *Adv. Mater. Res.* **415–417** 30
[3] Tsutaoka T, Kasagi T and Hatakeyama K 1999 *J. Eur. Ceram Soc.* **19** 1531
[4] Wang W J, Zang C G and Jiao Q J 2011 *Adv. Mater. Res.* **399–401** 310
[5] Grasset F, Labhsetwar N, Li D, Park D C, Saito N, Haneda H, Cador O, Roisnel T, Mornet S, Mornet S, Duguet E, Portier J and Etourneau J 2002 *Langmuir* **18** 8209
[6] Xie J L, Han M G, Chen L, Kuang R X and Deng L J 2007 *J. Magn. Magn. Mater.* **314** 37
[7] Shinde T J, Gadkari A B and Vasambekar P N 2013 *J. Magn. Magn. Mater.* **333** 152
[8] Nejati K and Zabihi R 2012 *Chem. Cent. J.* **6** 23
[9] Han M G and Deng L J 2013 *Chin. Phys. B* **22** 083303
[10] Yu G L, Li Y X, Zeng Y Q, Li J, Zuo L, Li Q and Zhang H W 2013 *Chin. Phys. B* **22** 077504
[11] Ren W J and Zhang Z D 2013 *Chin. Phys. B* **22** 077507
[12] Tian Y F, Hu S J, Yan S S and Mei L M 2013 *Chin. Phys. B* **22** 088505
[13] Roy P K and Bera J 2008 *J. Mater. Process. Tech.* **197** 279

[14] Dosoudil R, Ušáková M, Franek J, Grusková A and Sláma J 2008 *J. Magn. Magn. Mater.* **320** e849
[15] Han K C, Choi H D, Moon T J, Kim W S and Kim K Y 1995 *J. Mater. Sci.* **30** 3567
[16] Wang W J, Gumfekar S P, Jiao Q J and Zhao B X 2013 *J. Mater. Chem. C* **1** 2851
[17] Guo S L, Wang L D, Wang Y M, Wu H J and Shen Z Y 2013 *Chin. Phys. B* **22** 044101
[18] Kulkarni D C, Lonkar U B and Puri V 2008 *J. Magn. Magn. Mater.* **320** 1844
[19] Azadmanjiri J 2007 *J. Non-Cryst. Solids* **353** 4170
[20] Zahi S, Hashim M and Daud A R 2007 *J. Magn. Magn. Mater.* **308** 177
[21] Abbas S M, Dixit A K, Chatterjee R and Goel T C 2007 *J. Magn. Magn. Mater.* **309** 20
[22] Verma A, Saxena A K and Dube D C 2003 *J. Magn. Magn. Mater* **263** 228
[23] Singh P, Babbar V K, Razdan A, Puri R K and Goel T C 2000 *J. Appl. Phys.* **87** 4362
[24] Kim S S, Kim S T, Ahn J M and Kim K H 2004 *J. Magn. Magn. Mater.* **271** 39
[25] Zhu W B, Wang L, Zhao R, Ren J W, Lu G Z and Wang Y Q 2011 *Nanoscale* **3** 2862